ISSN 1674-1056
http://cpb.iphy.ac.cn
http://iopscience.iop.org/cpb
中国物理 B
Chinese Physics
中国物理
Chinese Physics B

Anti-detection technology of cat eye target based on decentered field lens

Da-Lin Song(宋大林), Jun Chang(常军), Yi-Fei Zhao(赵一菲), Ze-Xia Zhang(张泽霞)

Citation: Chin. Phys. B . 2018, 27(9): 094220. **doi:** 10.1088/1674-1056/27/9/094220

Journal homepage: http://cpb.iphy.ac.cn; http://iopscience.iop.org/cpb

What follows is a list of articles you may be interested in

Rapid measurement of transmission matrix with the sequential semi-definite programming method

Zhenfeng Zhang(张振峰), Bin Zhang(张彬), Qi Feng(冯祺), Huimei He(何惠梅), Yingchun Ding(丁迎春)

Chin. Phys. B . 2018, 27(8): 084201. **doi:** 10.1088/1674-1056/27/8/084201

Fabry-Pérot resonance coupling associated exceptional points in a composite grating structure

Zhi-Sen Jiang(蒋之森), De-Jiao Hu(胡德娇), Lin Pang(庞霖), Fu-Hua Gao(高福华), Ping Wang(王平)

Chin. Phys. B . 2018, 27(5): 054201. **doi:** 10.1088/1674-1056/27/5/054201

Broadband achromatic phase retarder based on metal-multilayer dielectric grating

Na Li(李娜), Wei-Jin Kong(孔伟金), Feng Xia(夏峰), Mao-Jin Yun(云茂金)

Chin. Phys. B . 2018, 27(5): 054202. **doi:** 10.1088/1674-1056/27/5/054202

Diurnal cooling for continuous thermal sources under direct subtropical sunlight produced by quasi-Cantor structure

Jia-Ye Wu(吴嘉野), Yuan-Zhi Gong(龚远志), Pei-Ran Huang(黄培然), Gen-Jun Ma(马根骏), Qiao-Feng Dai(戴峭峰)

Chin. Phys. B . 2017, 26(10): 104201. **doi:** 10.1088/1674-1056/26/10/104201

Simple and universal method in designs of high-efficiency diffractive optical elements for spectrum separation and beam concentration

Wen-Qi Xu(徐文琪), Dong-Feng Lin(林冬风), Xin Xu(许信), Jia-Sheng Ye(叶佳声), Xin-Ke Wang(王新柯), Sheng-Fei Feng(冯胜飞), Wen-Feng Sun(孙文峰), Peng Han(韩鹏), Yan Zhang(张岩), Qing-Bo Meng(孟庆波), Guo-Zhen Yang(杨国桢)

Chin. Phys. B . 2017, 26(7): 074202. **doi:** 10.1088/1674-1056/26/7/074202

Anti-detection technology of cat eye target based on decentered field lens*

Da-Lin Song(宋大林)[1,2], Jun Chang(常军)[1,†], Yi-Fei Zhao(赵一菲)[2], and Ze-Xia Zhang(张泽霞)[1]

[1] *School of Optics and Photonics, Beijing Institute of Technology, Beijing* 100081, *China*
[2] *The First Research Institute of the Ministry of Public Security, Beijing* 100048, *China*

(Received 25 February 2018; revised manuscript received 23 May 2018; published online 28 August 2018)

Optoelectronic imaging equipment is easy to expose to active laser detection devices because of "cat eye" effect. In this paper, we propose a new structure of optical system to reduce the retroreflector effect of a cat eye target. Decentered field lens structure is adopted in the design without sacrificing imaging quality and clear aperture. An imaging system with $\pm 30^{\circ}$ field of view is taken for example. The detailed design and simulation results are presented. The results indicate that this kind of optical system can reduce the retroreflection signal substantially and maintain acceptable imaging performance.

Keywords: geometric optical design, cat eye effect reduction, decentered field lens

PACS: 42.15.Eq **DOI:** 10.1088/1674-1056/27/9/094220

1. Introduction

Because of strong ability and high precision in detecting and capturing target images, the scouting, tracing, and measuring devices based on optoelectronic imaging are widely used. However, "cat eye" effect exists in most of imaging devices, leading to the retroreflection of incident light energy.[1,2] It is shown that the retroreflected light power is several times stronger than the power of diffusion target around. This cat eye effect is employed to scan, detect, and recognize an optoelectronic imaging equipment by the active laser detection technology.[3–5] The active laser detection devices are widely used in manportable, mobile, and onboard optoelectronic warning systems and possess good performance, and thus increasingly challenging the traditional optoelectronic imaging equipments.[6–13]

Some methods are proposed to reduce the retroreflection signal and cut down the effective range and identification probability of an active laser detection device. Defocusing method[14] can change the position of intersection point of reflected rays which are hence blocked by the lens diaphragm partly. But it will influence the imaging quality on the image sensor because of the departure from the optimal focus position. Camera tilting method can change the exit direction of the retroreflection rays and reduce the strength of reflected light to a certain extent. The more slanted the camera, the more the reflected energy that could be obscured. However, the seriously tilted image plane will induce large aberrations and also sacrifice the imaging quality. Another method is to use the band stop optical filter which will absorb the incident probe beam energy.[15] This method will not affect the imaging performance, but it can affect certain specific wavelengths only. An active laser detection device based on the wavelength tunable laser will abandon this method. An alternative way is to obscure part of the aperture stop.[16] The incident light entering the clear aperture will be blocked by the obscured part when it is retroreflected, hence no echo wave energy can be detected theoretically. Although this method has the potential to eliminate the cat eye effect completely, it reduces at least half of the pupil aperture in fact and affects the illuminance of image plane and diffraction limit of imaging lens. The above methods can reduce the cat eye effect of optoelectronic imaging system to an extent; however, they have limitations when put into practice.

Therefore, it is necessary to work out an improved scheme that has few influences on imaging performance but has an effect on more active laser detection device. In the present paper, we propose an ordinary and effective geometrical method in which a decentered field lens structure is adopted for reducing the retroreflection effect, and an example imaging system maintaining acceptable image quality is proposed. The simulation results are also shown subsequently.

2. Cat eye effect equivalent model

An ideal cat eye effect model can be equivalent to a combination of an imaging lens and a reflecting surface located on the focal plane[17] as shown in Fig. 1. As the detection beam irradiates the cat eye target, the laser ray will fill and enter into the lens entrance pupil. All the incident laser beam will be reflected along the direction that it originates from.

The laser echo power received by the receiving system

*Project supported by the National Natural Science Foundation of China (Grant No. 61471039).
†Corresponding author. E-mail: optics_chang@126.com
© 2018 Chinese Physical Society and IOP Publishing Ltd

detector can be described as[18]

$$P_r = \frac{0.838 P_0 A_S A_r \rho_s \tau_r^2 \tau^2 \tau_s^2}{(1/4\pi)^2 R^4 \theta_t^2 \theta_s^2}, \quad (1)$$

where P_0 is the laser output optical power, 0.838 is the percent of power distributed in the first obscure ring of Airy disc, A_S is the area of the receiver optics of the target, A_r is the area of the receiver optics of the detection system, ρ_s is the cat eye target reflectance, τ_r is the transmission of the optic receiver, τ is the transmission of the atmospheric path, τ_s is the transmission of the target transmitter optics, R is the distance between the detection system and the target, θ_t is the emitting beam divergence angle, and θ_s is the back-reflected laser divergence angle.

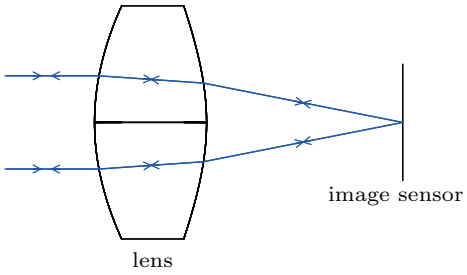


Fig. 1. (color online) Cat eye effect equivalent model layout including imaging lens and reflecting mirror.

3. Field lens decenter structure for eliminating retroreflection beam

If there exists a scheme in which the incident ray falling on the reflecting plane could be reflected by a completely different route, it will be able to find a way to block the reflected beam in an appropriate manner. A feasible way is to change the incident angle on the reflecting plane. As all the rays in an incident beam hit the reflecting plane on one side of optic axis as shown in Fig. 2, all the reflected rays will be traced only on the other side of the optic axis. And hence the desired effect could be achieved.

Considering that the field lens is commonly placed at or near the focal plane, the effect of the lens is to change the ray angle at the image plane, and hence reducing the clear aperture of the lens group behind usually. If placed exactly at the focus, it has little effect on the power and aberrations of the objective.

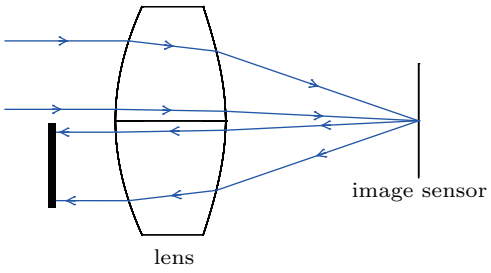


Fig. 2. (color online) Rays incident on one side of optic axis, thus reflected rays can be blokcked.

As shown in Fig. 3, d is a ray off-center distance relative to the optic axis of the field lens; u' is the deflection angle of the ray parallel to the optic axis, passed through the lens. It is easy to know that angle u' can be described in matrix notation as[19]

$$\begin{bmatrix} \tan(u') \\ d \end{bmatrix} = \begin{bmatrix} 1 & -\frac{1}{f} \\ 0 & 1 \end{bmatrix} \begin{bmatrix} 0 \\ d \end{bmatrix}, \quad (2)$$

where f is the focal distance of the field lens.

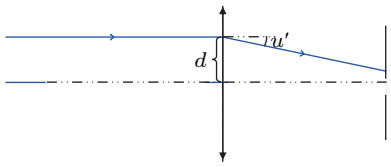


Fig. 3. (color online) Deflection of ray passed through field lens.

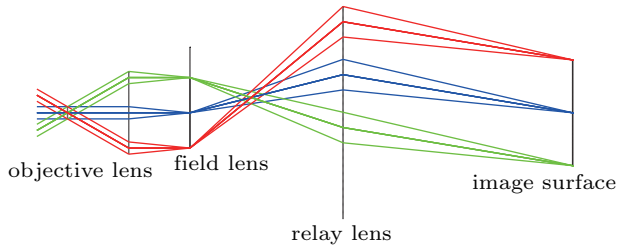


Fig. 4. (color online) Secondary imaging scheme including decentered field lens.

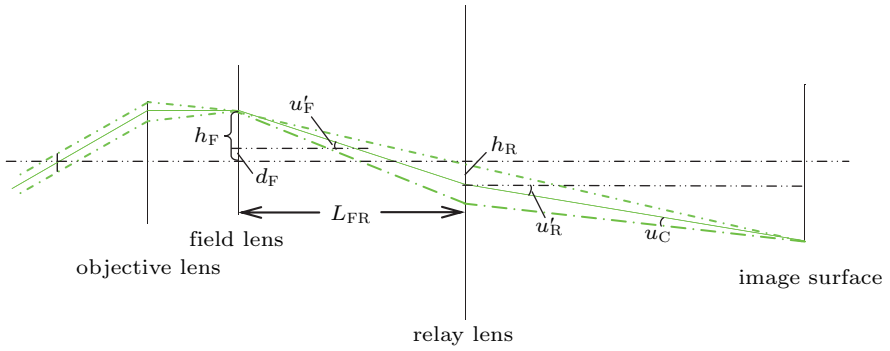


Fig. 5. (color online) Deflection of off-axis ray passed through decentered field lens.

If the field lens is decentered in the direction perpendicular to the axis, the deflection angle of the chief ray of each field of view will change a certain amount. Figure 4 shows a kind of secondary imaging scheme containing objective lens, field lens, and relay lens. The direction of incident rays is from left to right. In this optical structure, the objective lens and relay lens are both telecentric. For the chief ray of an arbitrary field of view as shown in Fig. 5, h_{F} is the intersection height on the field lens, d_{F} is the off-center magnitude of the field lens relative to the optical axis, h_{R} is the intersection height on the relay lens, u'_{F} is the refraction angle after the field lens and u'_{R} is the refraction angle after the relay lens.

For the field lens, the matrix notation can be described as[19]

$$\begin{bmatrix} -u'_{\mathrm{F}} \\ -(d_{\mathrm{F}}+h_{\mathrm{R}}) \end{bmatrix} = \begin{bmatrix} 1 & -\dfrac{1}{f_{\mathrm{F}}} \\ L_{\mathrm{FR}} & 1-\dfrac{L_{\mathrm{FR}}}{f_{\mathrm{F}}} \end{bmatrix} \begin{bmatrix} 0 \\ h_{\mathrm{F}}-d_{\mathrm{F}} \end{bmatrix}, \tag{3}$$

where f_{F} is the focal length of the field lens, and L_{FR} is the distance between the field lens and the relay lens. Because of the telecentric structure, the front focal plane of the relay lens and the rear focal plane of the field lens are coincident. So L_{FR} can be described as

$$L_{\mathrm{FR}} = f_{\mathrm{F}} + f_{\mathrm{R}}, \tag{4}$$

where f_{R} is the focal length of the relay lens.

For the relay lens, the matrix notation can be described as[19]

$$\begin{bmatrix} -u'_{\mathrm{R}} \\ -h_{\mathrm{R}} \end{bmatrix} = \begin{bmatrix} 1 & -\dfrac{1}{f_{\mathrm{R}}} \\ 0 & 1 \end{bmatrix} \begin{bmatrix} -u'_{\mathrm{F}} \\ -h_{\mathrm{R}} \end{bmatrix}. \tag{5}$$

Substituting Eqs. (3) and (4) into Eq. (5), the refraction angle can be described as

$$\tan u'_{\mathrm{R}} = \frac{d_{\mathrm{F}}}{f_{\mathrm{R}}}. \tag{6}$$

It can be seen that the incident angle of the chief ray of an arbitrary field of view on the image surface is related only to the off-center magnitude of the field lens and the focal length of the relay lens. Here the incident angle of the chief ray on the image surface u'_{R} is designed to be greater than the image cone angle u_{C}, as the off-center magnitude of field lens should meet

$$d_{\mathrm{F}} > \tan(u_{\mathrm{C}}) f_{\mathrm{R}}. \tag{7}$$

At this point, the reflected ray will go back along a completely different way from the incident ray, and can be blocked by the physical stop as shown in Fig. 6

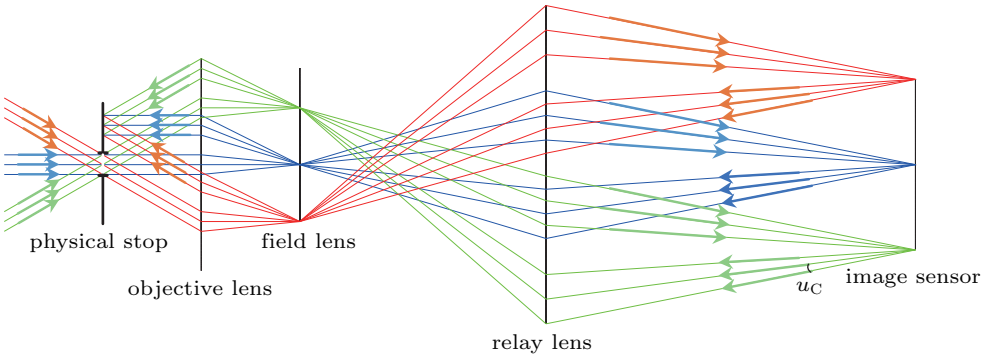


Fig. 6. (color online) Reflected rays going back in a completely different way from incident ray.

4. Utilization of decentered field lens structure in anti-detection imaging optical system

The accomplished system layout (as shown in Fig. 7) is the result of a stepwise design process. The field lens is decentered to meet the requirement for anti-detection function as analyzed in Section 3. The field lens and the relay lens group are both telecentric, which make each field of view satisfy the above requirement. Table 1 lists the design specifications. The ultimate value of modulation transfer function calculated by optical simulation software vs. field of view (field lens decentering direction) with decentered and coaxial field lens for 25 cyc/mm and 50 cyc/mm are shown in Fig. 8, and RMS spot radii before and after decentering the field lens are shown in Table 2, which indicates that the imaging performance degradation of the decentered structure is not significant.

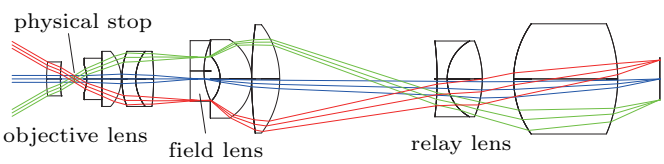


Fig. 7. (color online) Complete anti-detection imaging optical system.

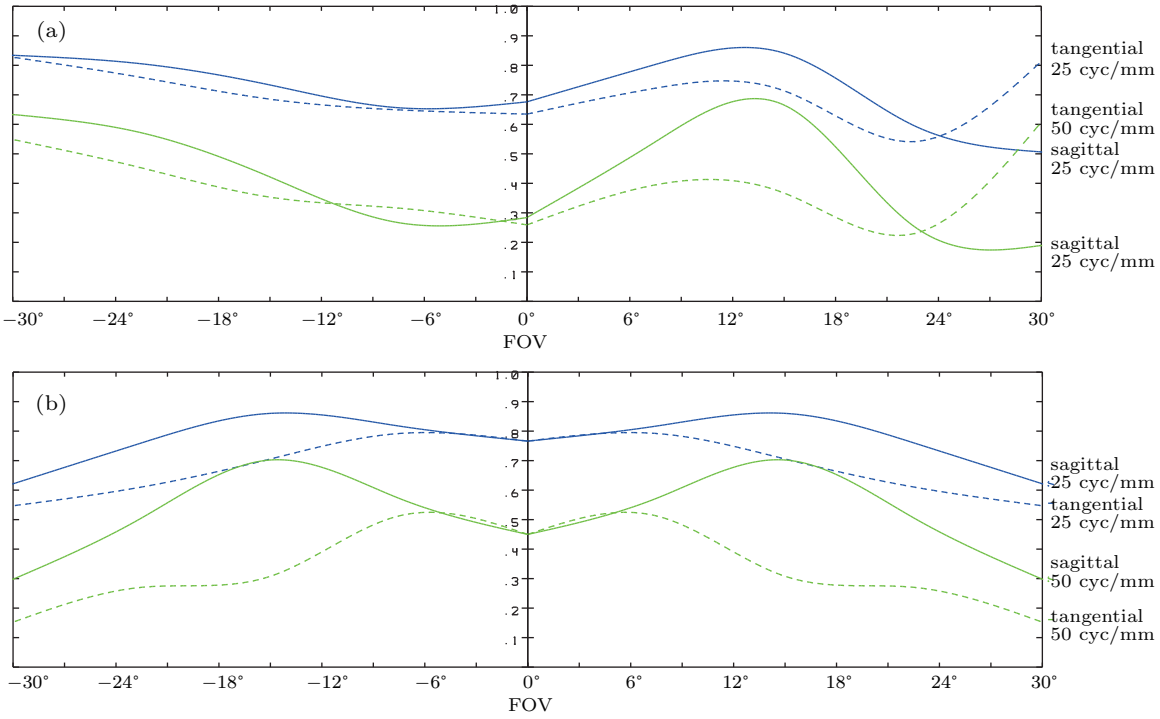


Fig. 8. (color online) Plots of modulation transfer function vs. field of view (direction of field lens decenter) with (a) decentered field lens and (b) coaxial field lens.

Table 1. Relevant specifications for designing anti-detection imaging optical system.

Focal length	6 mm
Field of view	±30°
$F/\#$	$F/6$
Spectral band	480–650 nm
Field lens decenter distance	1.15 mm

Table 2. RMS spot radius vs. field of view (direction of field lens decenter) with decentered field lens and coaxial field lens.

Field of view/(°)	RMS spot radius/μm	
	with decentered field lens	with coaxial field lens
–30	5.744	10.169
–20	6.252	6.850
–10	7.074	4.242
0	6.431	3.903
10	4.470	4.242
20	8.54	6.850
30	10.868	10.169
Equal weight average value	7.054	6.632

Next, the commercial optical illumination modeling software is used to simulate the detection procedure, and the results are shown in Fig. 9. In this model, the wavelength of the laser source is 632 nm, the diameters of the probe laser and receiver are the same as the entrance pupil of the lens, and the distance between the source laser and the imaging system is 15 times the focal length of the imaging lens. The reflectivity of the image sensor is set to be 10%, and the glass surfaces are coated with a quarter wave anti-reflection film.

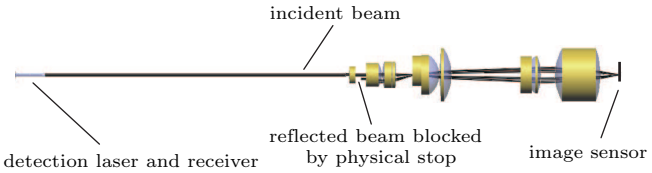


Fig. 9. (color online) Detection procedure simulating.

Figure 10 shows the simulation results, i.e., the plots of detection laser reflectivity versus field of view with the decentered and coaxial field lens respectively. The highest reflected value of laser with undecentered field lens is 7.99% appearing in 0° field of view, and the highest value with decentered field lens is 0.59% appearing in about 15° field of view, which is only 1/13.5 as much as the former. The data indicate that the field lens decentering scheme reduces the retroreflection signal substantially.

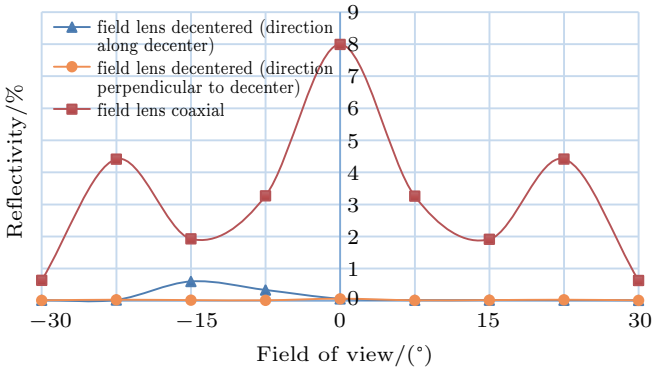


Fig. 10. (color online) Plots of laser reflectivity versus field of view with decentered and undecentered field lens.

5. Conclusion

We analyze and show the design of an anti-detection optical imaging system with field lens decentering scheme. The decentered field lens is an effective and practical way to reduce the cat eye effect. The value of modulation transfer function is greater than 0.2 at 50 cyc/mm across more than 70% of central field of view, and the average values of RMS spot radius for 7 fields of view before and after decentering the field lens are 6.632 μm and 7.054 μm, respectively. It indicates that the integral imaging quality degradation is little compared with the coaxial lens, and the field lens decentering scheme maintains acceptable imaging performance.

References

[1] Lecocq C, Ladobordowsky O and Meyzonnette J L 2003 *Proc. SPIE* **5086** 280
[2] Mieremet A L and Schleijpen R M A 2008 *Proc. SPIE* **2008** 6950
[3] Gong M, He S, Guo R and Wang W 2016 *Appl. Opt.* **55** 4461
[4] Rabinovich W S, Goetz P G, Mahon R, Waluschka E and Gilbreath G C 2003 *Proc. SPIE* **4975** 12
[5] Rabinovich W S, Goetz P G, Mahon R, Swingen L, Murphy J, Gilbreath G C and Binari S 2004 *Proc. SPIE* **5550** 12
[6] Sun H, Xiong F and Gu S 2006 *Proc. SPIE* **6344** 63442
[7] Sun H, Gu S and Ni G 2006 *Proc. SPIE* **6029** 334
[8] Wang Y, Zhang X, Wang L J and Wang C 2014 *Chin. Phys. B* **23** 014202
[9] Zhang C M, Ren W Y and Mu T K 2010 *Chin. Phys. B* **19** 024202
[10] Li C Y, Lu W G and Qiao L 2018 *Acta Phys. Sin.* **67** 030703 (in Chinese)
[11] Lu J N, Yu J and Tong Y Z 2012 *Chin. Phys. B* **21** 127105
[12] Wang D G, Deng Y Y, Zhang Z Y and Sun Y Z 2015 *Acta Phys. Sin.* **64** 060701 (in Chinese)
[13] Zhang X H, Zhang S and Sun C S 2016 *Acta Phys. Sin.* **65** 144204 (in Chinese)
[14] Zhang Y, Sun X, Lei P and Yu D 2015 *Infrared Laser Eng.* **44** 2268 (in Chinese)
[15] Liu B, Zhou B and Zhang Y 2012 *Semicond. Optoelectronics* **33** 121
[16] Arjan L M, Ric H M A S, Franc J M V P and Henny V 2010 *Opt. Eng.* **49** 1794
[17] Lei P, Xing H, Xue T and Lv H P 2009 *Infrared Laser Eng.* **45** 1084 (in Chinese)
[18] Sun H, Gu S and Ni G 2006 *Proc. SPIE* **6029** 334
[19] Smith W J 2000 *Modern Optical Engineering*, 3rd Edn. (New York: McGraw-Hill) pp. 54–55